Solar control of global mean temperature outweighed since 1940s by anthropogenic warming (by airborne soot, not CO2): literature synthesis

Roger Higgs

Geoclastica Ltd, UK

ABSTRACT

Primarily solar control of global warming and cooling for the last 9,000 years is proven by the striking likeness between published graphs of (1) average near-surface air temperature (from proxies and, since 1880, NASA-GISS thermometer data) and (2) solar-magnetic output. Graph-to-graph visual cross-matching of spikes and multi-century trends reveals a ~150-year temperature lag, attributable to ocean thermal inertia. The graphs clearly decouple in the 20th Century, 1940 to 2024 being disproportionately warm for the corresponding (time-lagged) solar output. Implicating humankind, this excess warmth coincides with the large growth, from World War Two onwards, in worldwide combustion of oil (aircraft, ships, vehicles) and coal (electricity production; steel- and cement-making). Further incriminating humans but *exonerating carbon dioxide (CO2)*, NASA's temperature graphs show that warming since 1985 is spatially inhomogeneous: much faster over land than ocean; faster in the Northern Hemisphere (land-ocean average) than the Southern; and nil in Antarctica (i.e. 'global warming' is not global). This spatial heterogeneity, at odds with CO2's globally homogenous atmospheric concentration, instead implicates airborne soot (absorbs solar radiation, thereby warming adjacent air), emitted mostly in the *northern-hemisphere* and *on-land*, mainly by burning coal, diesel-oil and wood (home-cooking by billions of people lacking electricity). Therefore, CO2's greenhouse effect is presumably offset by feedbacks underestimated or omitted in climate models (e.g. cloud effects fraught with uncertainty). Simply freezing world coal combustion at today's levels would halt airborne-soot growth, thus ending anthropogenic warming in ~10 years. Nevertheless, a sea-level rise of ~3 metres by 2100 appears inevitable (companion article by the author, in review). An even higher rise might be avoided by an urgent global shift from coal to natural gas (almost soot-free) for electricity generation. World gas reserves are sufficient for decades, giving

1

time for development of 'clean' (no soot or radioactive-waste), potentially limitless, nuclear-fusion energy.

1. Introduction

Climate scientists seldom look back beyond the establishment of reliable global thermometer network, in the 19th Century. A longer time-perspective is provided in this article, using proxy temperature- and solar-output data going back about 9,000 years, revealing that the Sun's magnetic-output fluctuations governed Earth's average temperature (Svensmark Theory) until very recently (20th Century). Integrating geological and astrophysical data covering thousands of years and 'fusing' them with meteorological and industrial (coal- and oil consumption data) spanning the last few decades and centuries can provide a better understanding of (a) the extent to which today's climate is 'overwarm', (B) when the extra warming began, and (c) what is the cause.

2. Methods

This contribution is solely based on the analysis, interpretation and synthesis of published information. No new data are presented, only ideas and interpretations.

3. Results

3.1. Global temperature largely solar-controlled prior to 1940

Published graphs of (1) solar-magnetic output (Wu et al., 2018) and (2) global near-surface air temperature (Marcott et al., 2013), both based on proxies spanning the last 9,000 years (Early to Late Holocene interglacial period), are visually alike, showing similar overall form and several cross-matching multi-century trends (rising, falling; Figure 1). However, the Marcott graph is heavily smoothed, due to averaging of 73 globally distributed datasets (diverse palaeotemperature proxies) and 1,000 Monte Carlo runs (Marcott et al., 2013). This smoothing suppresses short-term variability, rendering the graph less spiky, hampering correlation (Figure 1; note spikier reprocessed version by Vinos, 2017). This disadvantage is overcome here (Figure 2) by substituting a Greenland temperature graph (Vinther et al., 2009), which has the same general shape as the global graph (i.e. Greenland is a reasonable

2
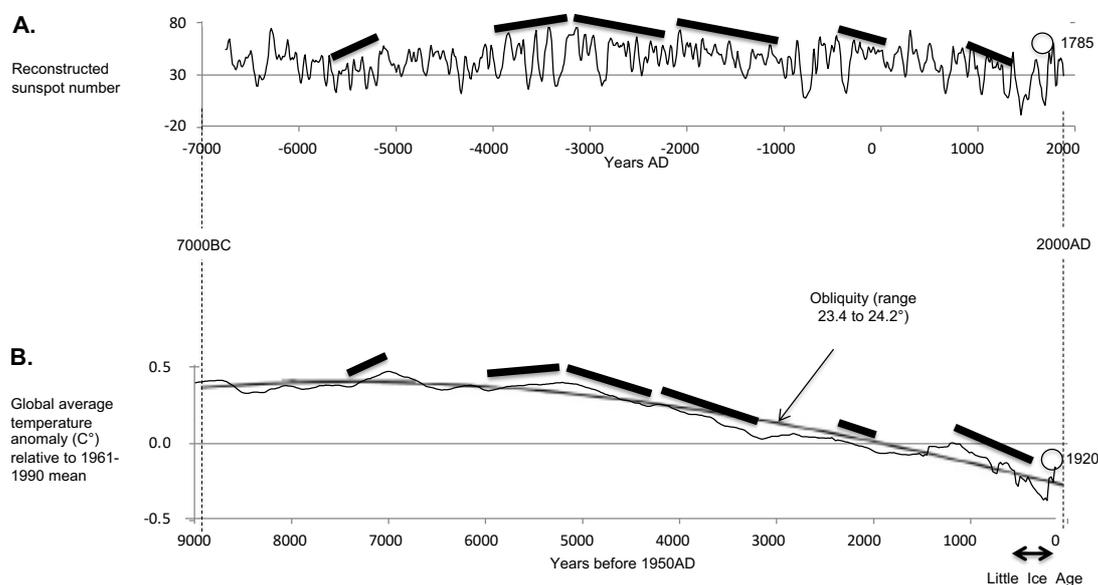
Figure 1. Visual correlation for the last 9,000 years between: (A) solar-magnetic output, based on proxy tree-ring ^{14}C and ice-core ^{10}Be, 10-year time-steps (too long to capture the basic 11-year solar cyclicity; e.g. Rohde, 2015; contrast Figure 5A), Wu et al. 2018 data at https://cdsarc.u-strasbg.fr/viz-bin/qcat?J/A+A/615/A93; (B) global average near-surface temperature anomaly relative to 1961-90 mean, based on multiple proxies, sampling resolution 20-500 years, 20-year time-steps, Marcott et al. (2013) data at https://www.science.org/doi/10.1126/science.1228026. In A and B, multi-century trends (rising, falling; black bars) match well. The similarity in shape of the two graphs is even clearer after tilting the temperature graph leftward to compensate for long-term cooling by Earth's declining axial obliquity (curved grey line, from Cionco et al., 2020). Marcott's final temperature value, for 1940, 0.7C° warmer than 1920, is omitted here, as he doubted its accuracy (see also Vinos, 2017).

world proxy; compare Figures 1B and 2B; Vinther dataset was among the 73 used by Marcott) but is much spikier thanks to minimal smoothing, as the graph is the average of only two, nearly identical, ice-core isotope profiles. A strong visual correlation between Greenland temperature and solar output is evident, with numerous cross-matching prominent spikes (peaks and troughs) and multi-century trends (Figure 2). The visual match can be further improved by rotating ('back-tilting') the temperature graph anti-clockwise, thereby compensating for long-term cooling by Earth's declining axial obliquity (smooth curve in Figure 2B). The match

3
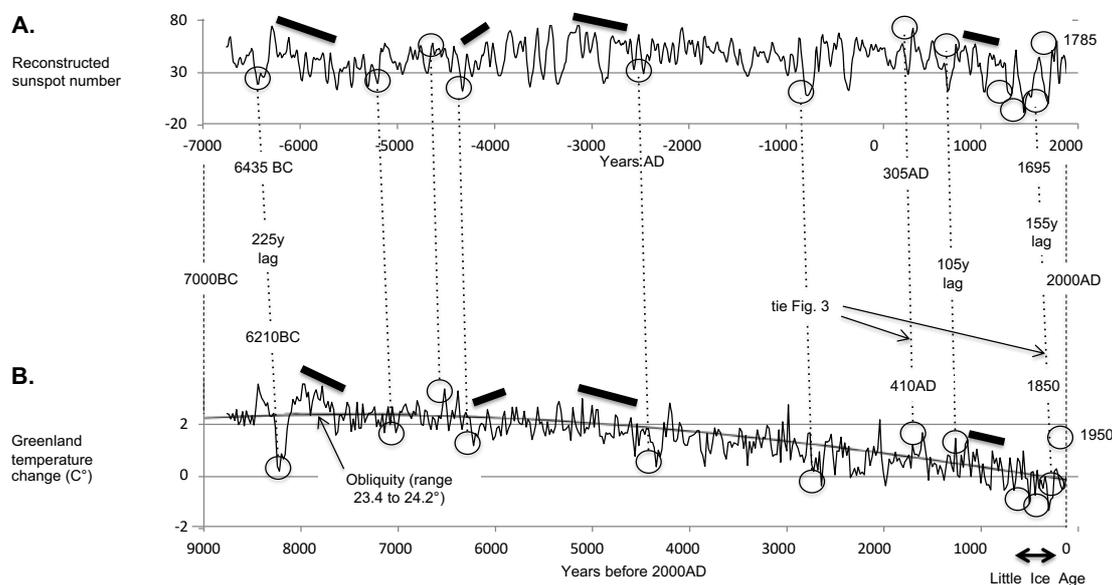
Figure 2. Visual correlation for the last 9,000 years between: **(A)** solar-magnetic output (same data-source as Figure 1A); and **(B)** Greenland near-surface air temperature change based on proxy ice-core ^{18}O, sample resolution 20 years, Vinther et al., 2009 data at https://www.ncei.noaa.gov/pub/data/paleo/icecore/greenland/vinther2009greenland.txt). Several prominent peaks and troughs (circled) and multi-century trends (black bars) match well. The match is even clearer after tilting the temperature leftward, compensating for long-term cooling by Earth's declining axial obliquity (curved black line, from Cionco et al., 2020). Slant of dashed correlation lines indicates that changes in temperature lag 100-250 years behind corresponding solar changes.

supports the Svensmark Theory that increased solar-magnetic output deflects more galactic cosmic rays, reducing cloudiness, allowing increased solar warming of the ocean (Svensmark, 2007), in turn warming the atmosphere. (The reverse assumption, by many climate scientists, that temperature-changes originate in the atmosphere and are transmitted to the ocean, was disproven by Humlum et al. [2013].) Notwithstanding the doubling of solar-magnetic flux from 1901 to 1992 (Lockwood et al., 1999), arguably to its highest level in >9,000 years (Solanki et al., 2004), the Intergovernmental Panel on Climate Change (IPCC) dismissed Svensmark's theory (Bindoff et al., 2013). Instead, the IPCC (2014, 2021a) estimated that the Sun has only a very small role in climate change, through (the very small) variations in total solar

4

irradiance (TSI), as opposed to magnetic-flux variations, which occur in lockstep with TSI but are far larger (e.g. see figure 1 of Benevolenskaya and Kostuchenko, 2013), e.g. the aforementioned doubling.

Non-matching spikes are also numerous (Figures 2, 3). Temperature spikes with no obvious solar counterpart include cold spikes, some attributable to terrestrial mega-eruptions (Sigl et al., 2015; Büntgen et al., 2016), and warm ones due to some other process(es), perhaps surges in submarine volcanism (i.e. lava eruptions and/or hydrothermal venting; cf. "plate climatology" of Kamis and Kamis, 2016), which is a hidden, unmeasurable, potentially major climate-change driver excluded in climate models (IPCC, 2014, 2021a). On the other hand, solar spikes lacking temperature expression might reflect submarine-heat surges or lulls counteracting the solar influence. The many non-matching solar and temperature spikes would result in a low mathematical correlation coefficient (after applying an oceanic time-lag; see below). Nevertheless, singular spectral analysis (SSA) of the 1850-2017 sunspot series and of the Hadley-CRU temperature data (see Section 3.2) "revealed modulated components that can reasonably be assigned to solar variability for most and even possibly all of them" (Le Mouël *et al.*, 2020, p. 24).

Simple visual cross-matching shows that temperature spikes lag 100 to 225 years behind corresponding solar spikes (Figure 2). The wide range of lag-times possibly reflects (1) dating errors (counting of tree rings and ice-core laminae), which increase with age, and/or (2) temporal variation in the oceanic lag-time. The longest lag (225 years) is between the exceptionally long solar grand minimum of ~6505-6365BC (Inceoglu et al., 2015) and the globally cold '8.2-kiloyear event' that spanned ~6250-6130BC in Greenland (Vinther et al., 2009 dataset), popularly attributed instead to hypothetical sudden emptying of an ice-dammed lake (Wikipedia, 2025a). Near the other (young) end of the graphs, the Little Ice Age (LIA) signature-cluster of three cold spikes is offset ~150 years from a trio of solar minima (Figure 2; NB middle spike of each triplet is the lowest value of the entire 9,000 years).

Focusing on the last two millennia (Figures 3, 4), the same solar graph (Wu et al., 2018) closely tracks the benchmark PAGES2k (2019) global multi-proxy temperature reconstruction. Cross-matched trends and spikes again reveal a temperature delay of ~150 years, e.g. the LIA (~1440-1920AD) corresponds to the triple Wolf-Spörer-Maunder solar minima (~1270-1760).

What causes the time-lag between solar output and global temperature (Figures 2-4)? An obvious candidate is ocean thermal inertia, i.e. the ocean's
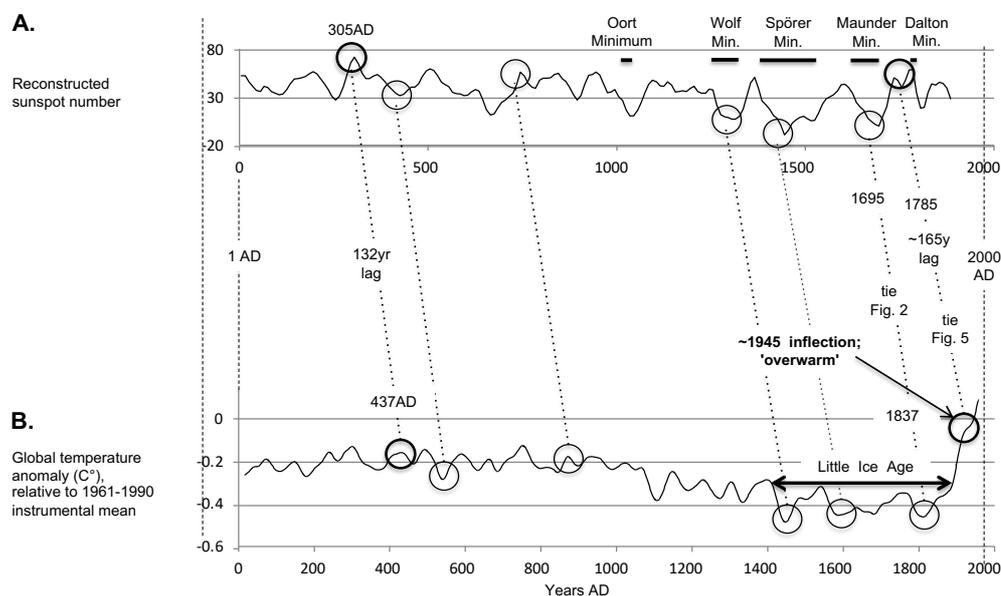
Figure 3. Visual correlation, for the last 2,000 years, between: **(A)** solar-magnetic output (same data-source as Figure 1A); and **(B)** global mean temperature, 1-year time-steps, 30-year smoothing, based on multiple proxies (tree rings, etc.), median of all reconstruction methods of PAGES2k (2019, fig.1a), their data at https://www.ncei.noaa.gov/access/paleo-search/study/26872. Solar minima from (e.g.) Steinhilber and Beer (2011). Several prominent peaks and troughs (circled) correspond well; slant of correlation lines indicates ~150-year lag, attributable to ocean thermal inertia (see text). The four bold circles demonstrate 1945AD disproportionate warmth, i.e. 437AD was cooler than 1945, despite *higher* corresponding solar activity (305AD) *and* higher obliquity (Figure 1 curved black line).

vastness, high specific heat and slow mixing render it slow to reach (transient) equilibrium. Summarising the results of modeling by himself and by others, Wigley (2005) said "Oceanic thermal inertia causes climate change to lag behind any changes in external forcing … many decades". This finding, despite the many assumptions and uncertainties inherent in all climate-related modelling, supports ascribing the ~150-year lag recognised here to ocean thermal inertia.

3.2. Solar control increasingly outweighed after 1940

      Remarkably, the solar- and temperature graphs very clearly 'decouple' in the 20th Century. Post-1940 warmth is disproportionately high, relative to the

6
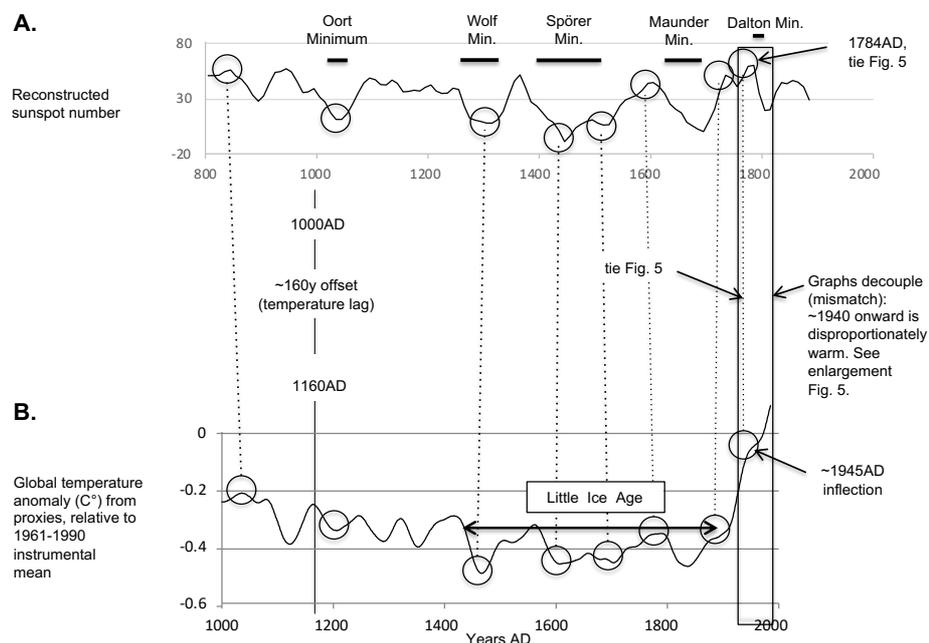
Figure 4. Time-shifted visual correlation, for the last 1,000 years, between: **(A)** solar-magnetic-output proxy; and **(B)** global mean temperature from proxies. Same data-sources as Figure 3. The best visual alignment of spikes (peaks, troughs; circled) is obtained by applying ~160-year temperature lag.

corresponding level of solar output (visually calibrated to previous episodes; Figures 3-5). To elucidate the 'excess' warmth, Figure 5 compares *thermometer*-measured 1880-2024 global average near-surface air temperature of NASA (2025; note that the NASA-GISS dataset is almost identical to the Hadley-CRU datasets [Met Office, 2025]) versus *annually* resolved 'solar modulation', a measure of solar-magnetic shielding of Earth from cosmic rays (Brehm et al., 2021). In Figure 5, global temperatures before 1940 closely mimic solar output after subtracting ~150-years lag, e.g. the three main temperature spikes (1898 warm, 1910 cold, 1942 warm) match three solar spikes (1740 high, 1750 low, 1784 high), moreover with equal proportionality. In contrast, post-1940 warming is excessive, manifested as follows: 1) 1942-56 cooling was overly weak for its corresponding solar decline (~150 years earlier), by comparison with previous similar declines (Figure 5, compare Box I and dashed box);

7
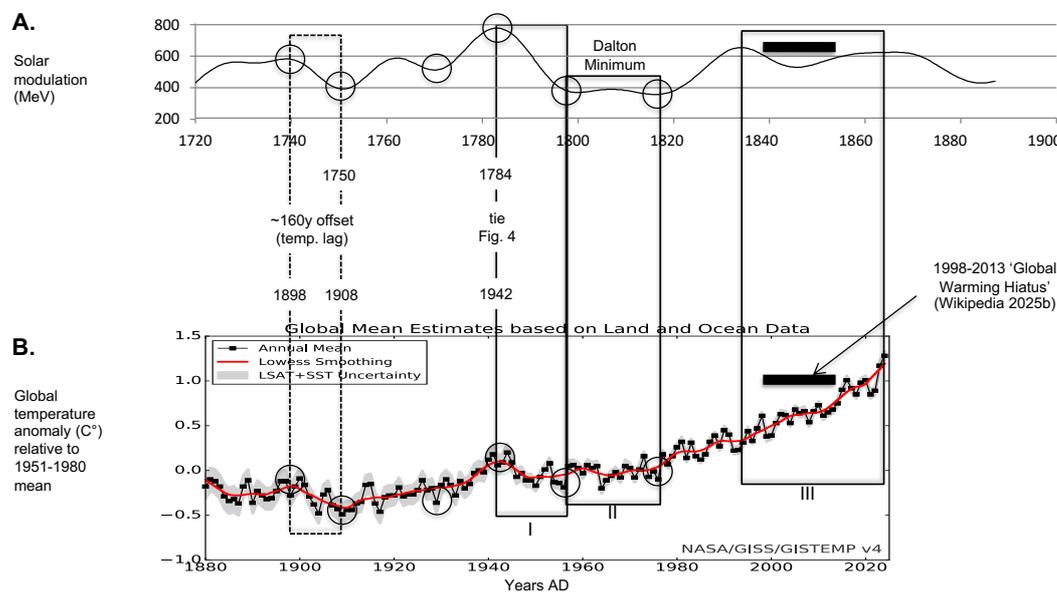
Figure 5. Visual correlation between**: (A)** 1720-1890 solar-magnetic output proxy, Brehm et al. 2021 20-year-smoothed annual tree-ring C14 data at https://www.nature.com/articles/s41561-020-00674-0; and **(B)** 1880-2024 global annual average near-surface-land-air and sea-surface temperature (NASA, 2025). Graphs are offset 160 years in accordance with Figures 2-4. Black boxes I-III highlight three manifestations of post-1942 excess temperature (relative to the corresponding solar output), as described in the text. Dashed box, see text. Five-year smoothed curve (red) suggests warming since 1975 is 'stepped' (cf. Figure 9).

2) therefore, the ensuing 1957-1975 interval of near-constant temperature (Box II), equating to the Sun's ~1800-1820 Dalton Minimum, was warmer than earlier times of *greater* corresponding solar strength (compare Box II and dashed box; see also Figure 3); and

3) 1995 to 2024 overall strong warming (despite the controversial 'Global Warming Hiatus', supposedly spanning 1998-2013 [Figure 5B; Wikipedia, 2025b]), anomalously equates to 1835-1865 net solar *decline* (involving a dip and a rise; Box III). This 1995-2024 warming is verified by satellite (Spencer, 2025), by balloon-radiosonde (Christy et al., 2018), and by Arctic sea-ice retreat (Stroeve et al., 2007; Mahoney et al., 2008; Connolly et al., 2017; Comiso et al., 2025).

8

Overall, 1940 to 2024 warming amounted to 1.1C°, despite a net *decline* in corresponding solar output (Figure 5).

3.3. *Human cause of post-1940 excess warmth*

Potentially incriminating humankind, the 1940 onset of excess warmth coincides with World War Two and its huge demand for coal (for producing electricity, steel and cement) and oil (aircraft, ships, vehicles). For example, the rate of world annual oil consumption doubled in 1940 (OWD, 2025a). Post-war rebuilding, industrial expansion and massive population growth (1950, 2.5 billion; 2020, 8 billion) have further increased oil- and coal demand.

Recognition of human culpability would implicate one or both of the potentially dominant causes of anthropogenic global warming, namely: (1) rising CO_2 emissions (from combustion of oil, gas, coal and wood), the overriding factor according to the IPCC (2014, 2021a, b) and to the great majority of climate scientists; and (2) airborne particulate 'black carbon' (Bond et al., 2013; Higgs, 2022, 2023), i.e. soot, mainly from combustion of diesel oil, coal and wood (Bond et al., 2013, table 8). In their landmark review of soot's estimated climatic effects, Bond et al. (2013, p. 5381) considered black carbon to be "the second most important human emission in terms of its climate forcing in the present-day atmosphere; only carbon dioxide is estimated to have a greater forcing". Soot deposited on ice and snow, lowering their albedo, was estimated to have only about one-fifth as much warming effect as airborne soot (Bond et al., 20213, table 1 and fig. 35).

Further incriminating humans, *but exonerating carbon dioxide* (CO2), meteorological evidence published mainly by NASA indicates that warming is laterally (geographically) and vertically inhomogeneous. The evidence includes:
1) lack of Antarctic warming since 1980 or earlier (Figure 6; Doran et al., 2002), i.e. 'global warming' is not truly global;
2) since 1985, faster near-surface warming over the continents than over the oceans, in contrast to pre-1985 near-lockstep warming and cooling (Figure 7C; NB sea-surface temperature is generally a good proxy for near-surface marine air temperature [Cayan, 1980; Rubino et al., 2020]);
3) faster warming since 1985 in the northern hemisphere (NH; land-ocean average) versus southern (SH) (Figure 8C);
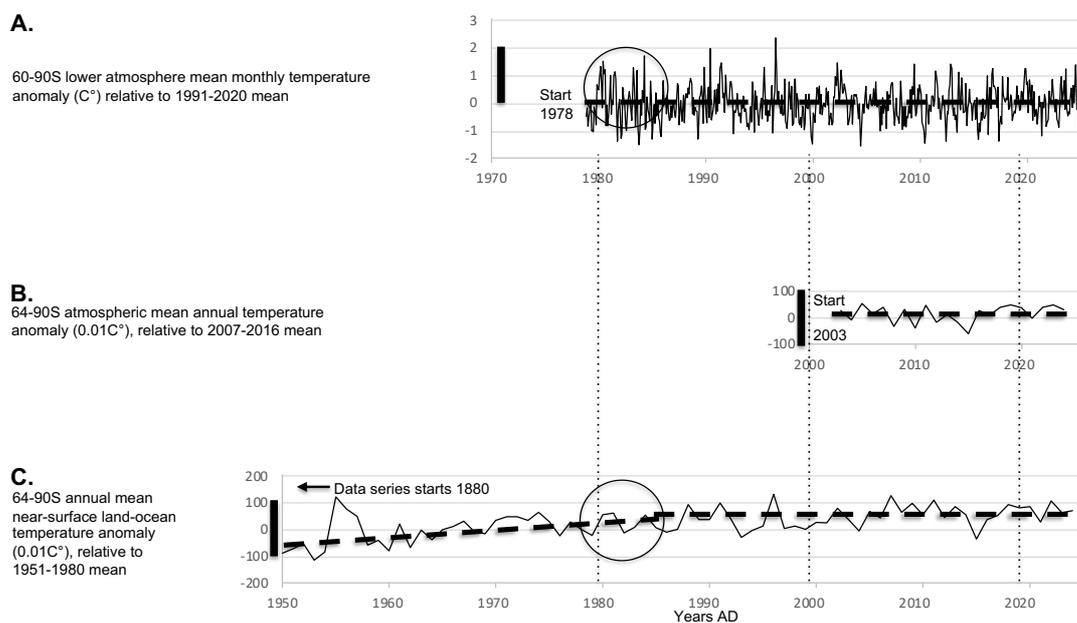
Figure 6. Three graphs (satellite and surface measurements) showing lack of warming in latitudinal belt 64-90S (Antarctica) since 1980. **(A)** Latitude 60-90S TIROS-N satellite-measured lower atmospheric monthly average temperature anomaly, 1978-2024, UAH data at https://www.nsstc.uah.edu/data/msu/v6.1/tlt/uahncdc_lt_6.1.txt. **(B)** 64-90S AIRS satellite-measured mean annual atmospheric temperature anomaly, 2003-2024, NASA data at https://data.giss.nasa.gov/gistemp/tabledata_v4/T_AIRS/ZonAnn.Ts+dSST.txt. **(C)** 64-90S mean annual near-surface-land-air- & sea-surface temperature anomaly, 1950-2024. NASA data (with "homogeneity adjustment") at https://data.giss.nasa.gov/gistemp/tabledata_v4/ZonAnn.Ts+dSST.txt. Vertical scales are equal (heavy bars indicate 1C°). Dashed bars are eyeballed average trends. Note lack of any obvious warming (or cooling) trend in any of the graphs since 1980, except in (C), which shows apparent overall warming from 1950 until ~1985, but the temperatures in the circled sector are relatively lower (down-shifted in the graph) than in (A), suggesting that the "homogeneity adjustment" is inappropriate.

4) faster lower-atmosphere warming (~0-9 km average, satellite-measured [UAH, 2025]) over continents than over ocean (Figure 7A, B; Klotzbach et al., 2009, table 1);

5) likewise NH versus SH (Figure 8A, B);

6) near-surface warming faster than lower-atmosphere warming, both over continents (Figure 7A, C) and over NH (Figure 8A, C); and

10

A.

Global over-land lower atmosphere mean monthly temperature anomaly (C°) relative to 1991-2020 mean

B.

Global over-ocean lower atmosphere mean monthly temperature anomaly (C°) relative to 1991-2020 mean

C.

Global mean near-surface land-air- (red) & sea-surface (blue) temperature anomaly (C°) relative to 1951-1980 mean
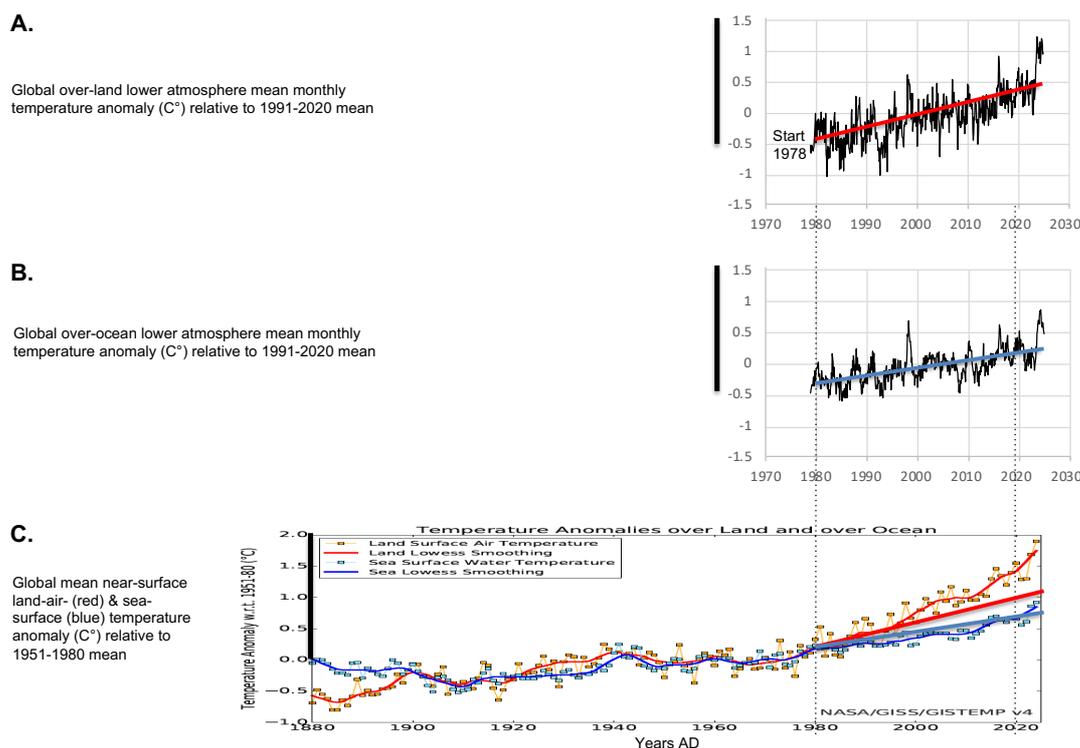
Figure 7. Comparison since 1978 of: (A) satellite-measured global lower atmospheric monthly average temperature anomaly over land and (B) ocean, same data source as Figure 6; and (C) near-surface global temperature anomaly over land (red) and ocean (blue), from NASA (2025). Vertical scales are equal; black bars = 2C°. Eyeballed red and blue trend-lines in A and B are transferred onto C for comparison. Atmospheric warming is greater over land (A) than over ocean (B). Note differential warming over land, i.e. less warming at altitude (A) than at surface (C). In contrast, there is no differential warming over ocean (B versus C), nor over Antarctica (Figure 6), nor the Southern Hemisphere (SH; Figure 8), confirming reliable 'calibration' of satellite- and surface instruments, and consistent with much less soot over oceans and SH than over land and NH (see text). Note, in C, terrestrial near-surface air has warmed faster than the sea-surface since 1985 (steeper gradient of wiggly red line), having previously been in lockstep.

7) near-surface warming at same rate as lower atmosphere over oceans (Figure 7B, C; Klotzbach et al., 2009, table 1) and over SH (Figure 8B, C). This observation verifies that surface (thermometer) and satellite measurements are well 'calibrated', as does their dual determination of non-warming in Antarctica (Figure 6).

The lateral and vertical warming gradients (observations 1 to 7 above) immediately exonerate CO2 because, being gaseous (molecular), CO2 disperses efficiently, producing near-homogenous atmospheric concentration, such that even heavily industrial regions barely (<0.5%) exceed the global average (Zhang et al.,

11

A.

NH lower atmosphere mean monthly temperature anomaly (C°) relative to 1991-2020 mean

B.

SH lower atmosphere mean monthly temperature anomaly (C°) relative to 1991-2020 mean

C.

Average near-surface NH (red) & SH (blue) temperature anomaly (C°) relative to 1951-1980 mean
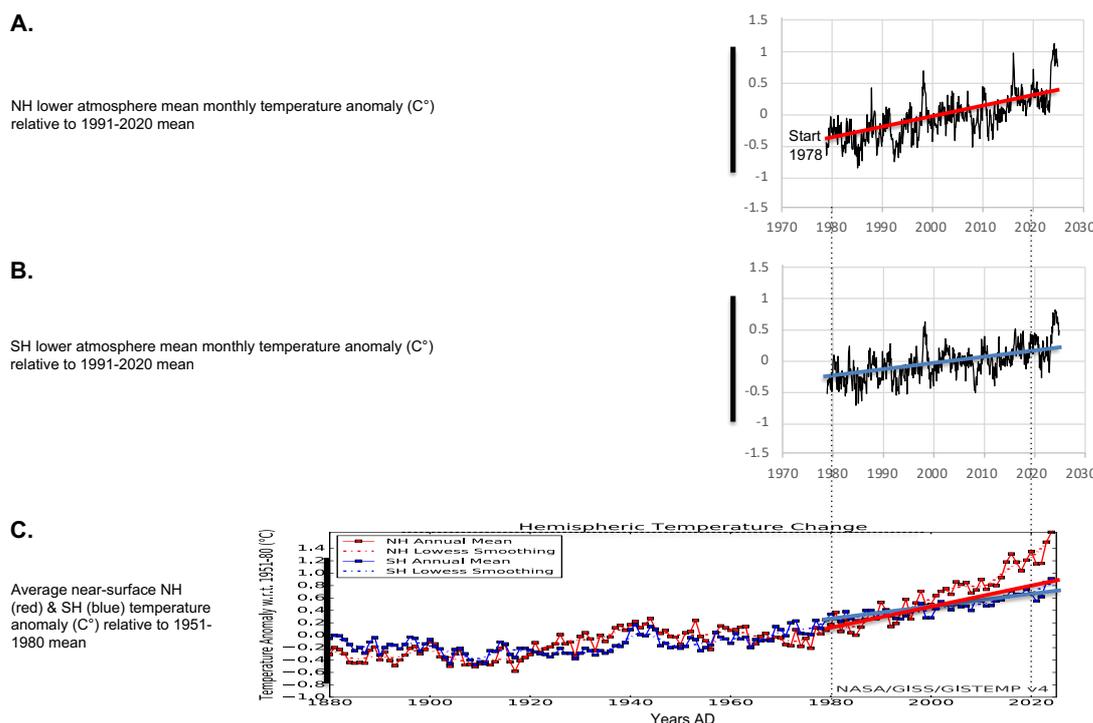
Figure 8. Comparison since 1978 of: (A) satellite-measured global lower atmospheric monthly average temperature anomaly over Northern Hemisphere (NH) and (B) Southern Hemisphere, same data source as Figure 6; and (C) near-surface global temperature anomaly over NH (red) and SH (blue), from NASA (2025). Vertical scales are equal; black bars = 2C°. Eyeballed trend-lines in A and B are transferred onto C for comparison. Atmospheric warming is greater over NH (A) than SH (B). Note differential warming over NH: less at altitude (A) than at surface (C). In contrast, there is no differential warming over SH (B versus C). Note, in C, NH has warmed faster than SH since 1985 (steeper gradient of wiggly red line), having previously been in lockstep.

2019, fig. 1). If CO2 were really Earth's "temperature control knob" (Lacis et al., 2010), modern warming would be much more uniform areally. Instead, the gradients incriminate airborne soot because, being particulate, it disperses much less efficiently, remaining concentrated near its mainly *land-based*, *northern-hemisphere* sources (e.g. Allen et al., 2012, fig. 1a). (Antarctica soot emissions are minimal, but see Cordero et al. [2022].)

Airborne soot was similarly credited with major climatic importance by Allen et al. (2012), who attributed northward expansion of the tropical belt in recent decades to laterally heterogenous atmospheric warming by soot (and ozone). "Owing to increased combustion of fossil fuels and biofuels, black carbon aerosols

have increased substantially over much of the Northern Hemisphere during the last few decades, particularly over southeast Asia ... black carbon has increased monotonically since 1970 on average in the low and midlatitudes, including the band 30°-50° N ... where recent studies show that heating can displace the tropical edge" (Allen et al., 2012, p. 350-351) ... "Our analysis strongly suggests that recent Northern Hemisphere tropical expansion is driven mainly by black carbon and tropospheric ozone, with greenhouse gases playing a smaller part" (p. 352). In a follow-up article, Zhao et al. (2020, p. 1) added: "Our results show that ... black carbon (BC) aerosol drives tropical expansion ... BC, especially from Asia, is more efficient ... than greenhouse gases in driving tropical expansion ... Although a formal attribution is difficult, scaling the normalized expansion rates to the historical time period suggests that BC is the largest driver of the Northern Hemisphere tropical widening but with relatively large uncertainty. ... BC warms the troposphere, particularly in the NH midlatitudes where most emissions occur."

Soot is produced primarily by the burning of three commodities (Bond et al., 2013, table 8): oil-derived fuels (in cars, buses, trucks, ships, aircraft), especially diesel; coal (mainly in powerplants, steelworks and cement plants); and wood (home cooking by billions of people lacking electricity). The settling soot particles are black, hence solar radiation warms them (Jacobson, 2001), in turn warming the surrounding air. Over intensely industrialized regions (e.g. eastern USA, Europe, China), average atmospheric soot concentration is approximately 1000% (i.e. 10 times) greater than over adjacent oceans (NASA, 2011), in contrast to CO_2's roughly 1% difference (NASA, 2016). Soot also has a strong *vertical* concentration gradient, explaining the slower warming at altitude (observation 6, above), e.g. global average approximately 100 times greater at 1 km than at 10 km (Cooke et al., 1999, fig. 10), in stark contrast to CO_2, only 4% less at 4 km than at 1 km above Tokyo (Shibata et al., 2018, fig. 6).

Further evidence of airborne-soot's culpability comes from plotting post-1860 coal- and oil production alongside land- and ocean warming (Figure 9). Applying a 10-15-year temperature lag provides not only a good visual match but also a logical inter-relation of three details of the three charts in Figure 9, as follows:
1) 1960 tripling of oil growth-rate equates to 1975 renewal of warming (both land and ocean);

13
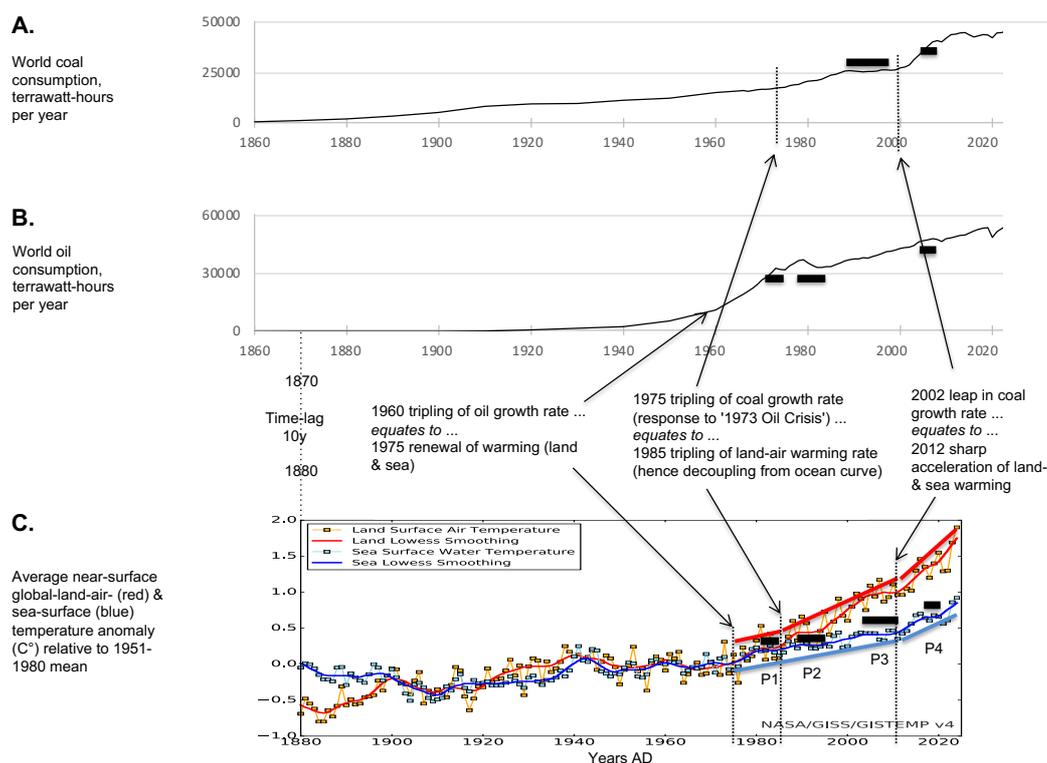
Figure 9. Comparison of 1880 to 2024 (A) global coal consumption, (B) oil consumption, and (C) global average near-surface land-air- versus sea-surface temperature anomaly. Data for (A) and (B) from OWD (2025a); data-points are every tenth year until 1960 and annual from 1965 onward. (C) from NASA 2025. Four warming-pauses (black bars P1 to P4) give both temperature curves in (C) a 'stairstep' appearance. Applying a 10-15-year temperature lag, by shifting (C) to the right, provides a good visual match among all three charts, and a logical inter-relation of their details (see annotations), and also aligns the pauses (P1 to P4) with times of zero- or negative growth of coal- and/or oil consumption (unlabelled black bars).

2) 1975 tripling of coal growth-rate (in response to '1973 Oil Crisis', e.g. Wikipedia) equates to 1985 tripling of land-air warming rate (hence decoupling from ocean curve; Figure 7C); and

3) 2002 leap in coal growth-rate equates to 2012 sharp acceleration of NH and SH warming. Similar probable cause-and-effect relationships are seen with the NH versus SH temperature graph (Figure 10). The lag also aligns four warming pauses (P1 to P4 in Figure 9C, 3-7 years each) with times of zero or negative growth of coal- and/or oil consumption (Figure 9A, B). The warming pauses do not match CO2's smooth, slightly accelerating, uninterrupted rise (no 'stairsteps'; Figure 11). In

14
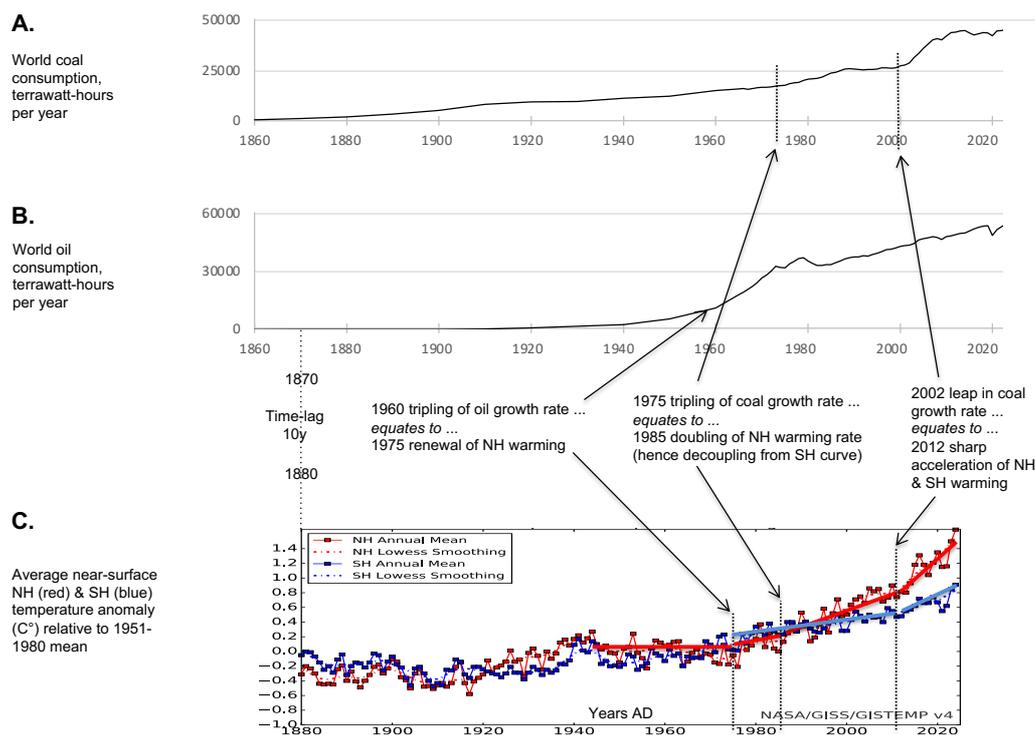
Figure 10. Comparison of 1880 to 2024 (A) global coal consumption, (B) oil consumption, and (C) Northern Hemisphere (NH) versus Southern (SH) mean annual temperature anomaly. Data source for (A) and (B) same as Figure 9. (C) from NASA 2025. Applying a 10-15-year temperature lag, by shifting (C) to the right, provides a good visual match among all three charts, and a logical inter-relation of their details (see annotations).

contrast, the stepped rise in global coal- and oil consumption mimics the 'stairstep' warming (Figure 9).

In the literature, soot's contribution to atmospheric warming is very uncertain. According to Bond et al. (2013, p. 5388, italic emphasis added here): "The best *estimate* of industrial-era climate forcing of black carbon ... is +1.1 W m-2 with 90% *uncertainty bounds* of +0.17 to +2.1 W m-2 [sic; see also their table 1 and fig. 35] ... We *estimate* that black carbon ... is the second most important human emission in terms of its climate forcing", after CO2. Black carbon's warming effect was *estimated* to be 70% as strong as CO2 (p. 5497). Recent IPCC *estimates* are much lower, about 35% and 20%, again with large uncertainties (2013, fig. SPM.5; 2021a, fig. SPM.2c). In contrast, the data presented above suggest that soot is by far the dominant agent of anthropogenic warming.
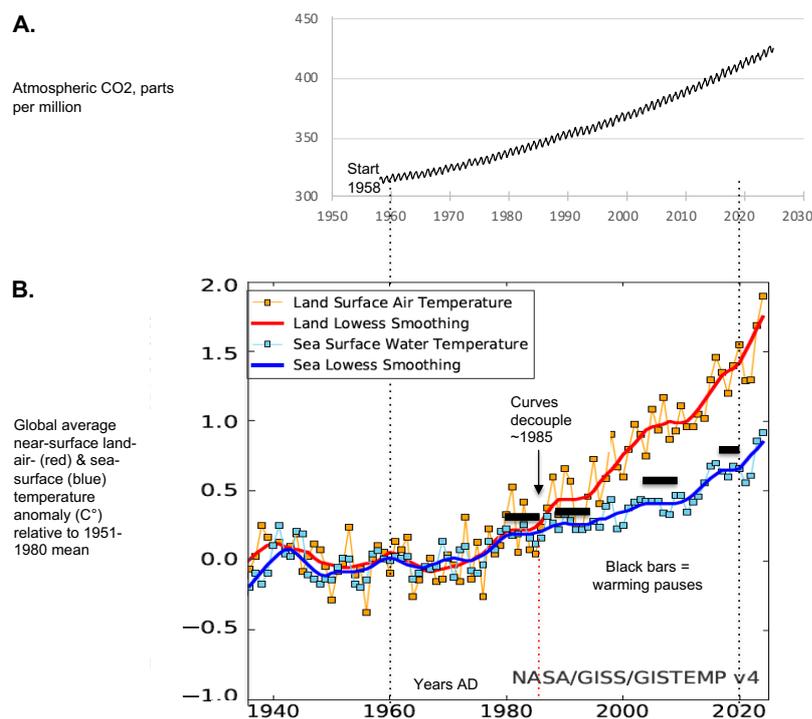
Figure 11. Comparison of (A) monthly average atmospheric CO2 concentration (note seasonal fluctuation), from https://gml.noaa.gov/ccgg/trends/data.html and (B) global average near-surface land-air- and sea-surface temperature anomaly (NASA, 2005). In (A), CO2's smooth (slightly accelerating) uninterrupted rise in cannot explain, in (B), the decoupling (~1985) of land- and sea temperature curves, or their 'stepped' nature (reflecting warming hiatuses; Figure 9).

Besides the effect of airborne soot, some of the excess (anthropogenic) warmth may be 'waste heat' (thermal pollution by power stations, air conditioners, etc.), considered by some to be an important (Chen et al., 2014), or dominant (Bian, 2020), or overwhelming (Karamanev, 2021) source of warming.

3.4. Reasons for underestimation of soot effect and overestimation of CO2 effect

Helping to explain previous underestimates of soot's warming effect, developing-world powerplants possibly emit far more soot than the Bond et al. (2013) review assumed. Coal is still the dominant fuel for world electricity generation (35%; OWD, 2025b). Bond et al. (2013) estimated global coal-fired-powerplant soot emissions to be relatively low (20 Gg/yr, their table 8), because "the high temperatures and well managed combustion promote burnout of any BC [black carbon] that is formed" (p. 5414). But the next sentence admitted "emission rates

16

from power generation in developing countries are not well known" (p. 5414). Bond et al. (2013) then cited Cooke et al. (1999) as estimating global soot emissions ~80 (sic) times higher (an increase of 1600 Gg/yr; p. 5414), and continued "there remains a persistent but informal perception ... that BC fractions of particulate matter in developing countries, especially in power plants and industrial installations, could be higher than that represented by existing measurements. Even if older, poorly operating power plants have high BC emission factors, there is no evidence that newly installed, modern power plants do" (p. 5414-15).

Another possible reason for airborne soot having a greater impact on climate than previously supposed is underestimation of soot's effects on clouds. Bond et al. (2013, fig. 35) estimated the net (combined) effect of these positive and negative feedbacks to be positive, but with very large uncertainties. Subsequently, Lohmann et al. (2020) stressed the importance of soot-induced cloud-related positive feedbacks.

The above evidence of CO_2's negligible effect on temperature implies that its greenhouse effect, already reduced "well into the saturation regime" (van Wijngaarden and Happer, 2020, p. 18), is nullified by negative feedbacks omitted or underestimated in climate models. For example, cloud feedbacks are highly uncertain (Stephens, 2005). IPCC (2013, p. 14) admitted "aerosols and their interactions with clouds have offset a substantial portion of global mean forcing from ... greenhouse gases. They ... contribute the largest uncertainty". IPCC (2014, p. 44) stated: "The radiative forcing from aerosols, which includes cloud adjustments ... has two competing components: a dominant cooling effect from most aerosols and their cloud adjustments and a partially offsetting warming contribution from black carbon absorption of solar radiation. There is high confidence that the global mean total aerosol radiative forcing has counteracted a substantial portion of radiative forcing from well mixed GHGs [greenhouse gases]. Aerosols continue to contribute the largest uncertainty to the total radiative forcing estimate". In its next (6th) major report, the most recent, IPCC (2021b, p. 95) confessed "clouds remain the largest contribution to overall uncertainty in climate feedbacks" but nevertheless concluded that "The net effect of changes in clouds in response to global warming is to amplify human-induced warming, that is, the net cloud feedback is positive (*high confidence*)" (their italics).

One CO_2-related feedback that is almost certainly negative is the increase in "Biogenic volatile organic compounds (BVOCs) ... potentially very important"

17

(Kulmala et al., 2013, p. 498), caused by faster forest growth thanks to both fertilization by rising CO2 and warming. According to the IPCC (Szopa et al., 2021), "BVOCs are emitted in large amounts by forests and ... in a warming planet ... are expected to increase but magnitude is unknown and will depend on future land-use change, in addition to climate (*limited evidence, medium agreement*)" (their italics; p. 825). The "evaluation of global BVOC emissions is challenging because of poor measurement data coverage in many regions and the lack of year-round measurements. ... Most CMIP6 models use overly simplistic parametrizations and project an increase in global BVOC emissions in response to warming temperatures ... [but] ... do not fully account for the complex processes influencing emissions ... that are hard to constrain observationally" (p. 831). The "assessed central estimate of the climate-BVOC feedback ... suggests that climate-induced increases in SOA [secondary organic aerosols] from BVOCs will lead to a strong cooling effect that will *outweigh the warming from increased ozone and methane lifetime* [italics added here; no mention of potentially outweighing CO2 greenhouse effect], however the uncertainty is large" (p. 859). Given all of the uncertainties expressed by the IPCC, and the evidence presented above for CO2's innocence, it seems likely that climate models favoured by the IPCC have underestimated BVOC negative feedback.

Further evidence for CO2's blamelessness comes from Murray and Heggie (2016), who found that 1965-2013 warming in the United Kingdom and Japan correlate better with national energy consumption, "a proxy for thermal emission" (i.e. waste heat), than with CO2-based climate models. However, both the UK and Japan relied heavily on oil-fuels and coal for their total energy requirements (electricity, transport, heating) in that time period (OWD, 2025a), therefore energy consumption is also a proxy for airborne soot.

4. Discussion: climate and sea-level in the coming decades

If soot is indeed the principal anthropogenic warming agent, then stopping global warming is technically (but not politically) easy: simply freezing global oil- and coal combustion at today's levels would halt airborne-soot growth, thereby halting anthropogenic warming in about 10 years (lag-time in Figure 9). Going further and *reducing* consumption would cause cooling. However, in reality, consumption will keep rising, as developing nations strive to grow their economies and their armed forces. For example, from 2005 to 2023, China's coal usage grew 65%

18

while the UK's shrank 90% (OWD, 2025a). In 2023, China, with 20 times the UK population, burned 500 (sic) times as much coal. Moreover, the exceptional doubling of solar-magnetic output from 1901 to 1992 (Lockwood et al., 1999, fig. 3; note 1992 cosmic-ray strong minimum of Oulu, 2025), to its highest level in >2,000 years (Wu et al., 2018, fig. 14, red peak 1992), means that strong Sun-driven warming will start adding to anthropogenic warming after ~2060, with a peak contribution ~2150 (~160-year lag, Figures 4, 5).

If future climate-modelling confirms that CO_2 plays no role in global warming, governments should urgently implement appropriate measures toward ending anthropogenic warming, thereby *perhaps* also preventing sea-level rising much more than 3m. (Unfortunately, even if warming were stopped today, a sea-level rise of at least 3m now appears inevitable [Higgs, 2024 and manuscript in review]). Establishing that the true 'enemy' is soot, not CO_2, would justify generating much more of the world's electricity using natural gas (only 22% in 2023), which emits CO_2 but almost no soot when properly combusted. New gas-fired capacity could replace existing coal (36%) and nuclear-fission powerplants (9%), with the additional double-benefit of improving air quality and halting further radioactive-waste production. Confirmation of CO_2's innocence would render wind turbines (8%) and solar panels (5%) triply indefensible: intermittent; 'commandeer' priceless land (agriculture, housing, natural habitats, aesthetic beauty); vast disposal problem (most going to landfill). Planned 'carbon capture' would become triply mistaken: needless; waste of trillions of dollars; will retard CO_2-fertilisation of crops and forests. (At 425ppm in early 2025, CO_2 is still only about 40% of the ~1,000ppm optimum for plant growth [e.g. Zheng *et al.*, 2018], and is exceptionally low in terms of the last 500 million years [e.g. Berner and Kothavala, 2001]).

If soot is indeed the main culprit and CO_2 entirely innocent, it is suggested here that no new coal-, wind-, solar-, or nuclear-fission powerplants be built, only gas-fired ones. Global proven gas reserves would last about 50 years at the current consumption rate (OWD, 2025c), or 25 years at twice that rate. 'Probable reserves', which automatically become 'proven' as soon as higher prices render them economically recoverable, would last for additional decades. Perhaps limitless, 'clean' (no soot or radioactive-waste), nuclear-*fusion* energy will be a reality by then.

References

Allen, R.J., Sherwood, S.C., Norris, J.R. and Zender, C.S., 2012. Recent Northern Hemisphere tropical expansion primarily driven by black carbon and tropospheric ozone. Nature, v. 485, p. 350-355, https://www.nature.com/articles/nature11097

Benevolenskaya, E.E. and Kostuchenko, I.G., 2013. The total solar irradiance, UV emission and magnetic flux during the last solar cycle minimum. Journal of Astrophysics, v., 2013, article 368380, https://doi.org/10.1155/2013/368380

Berner, R.A. and Kothavala, Z., 2001. GEOCARB III: a revised model of atmospheric CO2 over Phanerozoic time. American Journal of Science, v. 301, p. 182–204, https://ajsonline.org/article/61570

Bian, Q., 2020. Waste heat: the dominating root cause of current global warming. Environmental Systems Research, v. 9, article 8, https://doi.org/10.1186/s40068-020-00169-2

Bindoff, N.L. and 14 others, 2013. Chapter 10, Detection and attribution of climate change: from global to regional. *In:* Stocker, T.F., and 9 others, eds., Climate Change, 2013: The Physical Science Basis. Contribution of Working Group I to the Fifth Assessment Report of the Intergovernmental Panel on Climate Change. Cambridge University Press, Cambridge UK and New York USA, p. 867-952, https://www.ipcc.ch/site/assets/uploads/2018/02/WG1AR5_Chapter10_FINAL.pdf

Bond, T.C. and 30 others, 2013. Bounding the role of black carbon in the climate system. a scientific assessment. Journal of Geophysical Research: Atmospheres, v. 118, p. 5380-5552, https://doi.org/10.1002/jgrd.50171

Brehm, N. and 13 others, 2021. Eleven-year solar cycles over the last millennium revealed by radiocarbon in tree rings. Nature Geoscience, v. 14, p. 10-15, https://doi.org/10.1038/s41561-020-00674-0

Büntgen, U. and 15 others, 2016. Cooling and societal change during the Late Antique Little Ice Age from 536 to around 660 AD. Nature Geoscience, v. 9, p. 231-236, https://doi.org/10.1038/ngeo2652

Cayan, D.R., 1980. Large-scale relationships between sea surface temperature and surface air temperature. American Meteorological Society, Monthly Weather Review, v. 108, p. 1293-1301, https://doi.org/10.1175/1520-0493(1980)108<1293:LSRBSS>2.0.CO;2

Chen, B., Dong, L., Shi, G., Li, L.-J. and Chen, L.-F., 2014. Anthropogenic heat release: estimation of global distribution and possible climate effect. Journal of the Meteorological Society of Japan, v. 92A, p. 157-165, https://doi.org/10.2151/jmsj.2014-A10

Christy, J.R., Spencer, R.W., Braswell, W.D. and Junod, R., 2018. Examination of space-based bulk atmospheric temperatures used in climate research. International Journal of Remote Sensing, v. 39, p. 3580-3607, https://doi.org/10.1080/01431161.2018.1444293

Cionco, R.G., Soon, W. W-H. and Quaranta, N.E., 2020. On the calculation of latitudinal insolation gradients throughout the Holocene. Advances in Space Research, v. 66, p. 720-742, https://doi.org/10.1016/j.asr.2020.04.030

Comiso, J.C., Parkinson, C.L., Gersten, R., Bliss, A.C. and Markus, T. , 2025. Current state of sea ice cover. Webpage accessed 18th January 2025, https://earth.gsfc.nasa.gov/cryo/data/current-state-sea-ice-cover

Connolly, R., Connolly, M., and Soon, W. 2017. Re-calibration of Arctic sea ice extent datasets using Arctic surface air temperature records. Hydrological Sciences Journal, v. 62, p. 1317-1340, https://doi.org/10.1080/02626667.2017.1324974

Cooke, W.F., Liousse, C., Cachier, H. and Feichter J. 1999. Construction of a 1° x 1° fossil fuel emission data set for carbonaceous aerosol and implementation and radiative impact in the ECHAM4 model. Journal of Geophysical Research, v. 104, p. 22,137-22,162, https://agupubs.onlinelibrary.wiley.com/doi/abs/10.1029/1999jd900187

Cordero, R.R., and 20 others, 2022. Black carbon footprint of human presence in Antarctica. Nature Communications, 13:984, https://doi.org/10.1038/s41467-022-28560-w

Doran, P.T. and 12 others, 2002. Antarctic climate cooling and terrestrial ecosystem response. Nature, v. 415, p. 517-520, https://www.nature.com/articles/nature710

Higgs, R., 2022. Solar control of global temperature outweighed since 1940 by anthropogenic warming (by waste heat and black carbon, not CO2?). Geological Society of America, Annual Meeting, Denver, Colorado, abstract and poster, https://gsa.confex.com/gsa/2022AM/webprogram/Paper380198.html

Higgs, R., 2023. Global warming spatial inequality (land warming much faster than sea since 1985) incriminates soot from burning coal, exonerates CO2. European Geosciences Union (EGU), General Assembly, 2023, Vienna, abstract and poster, https://doi.org/10.5194/egusphere-egu23-1416

Higgs, R., 2024. British archaeology verifies 5th-Century rapid multi-metre sea-level rise and portends another before 2100. European Geosciences Union (EGU), General Assembly, 2024, Vienna, abstract and poster, https://doi.org/10.5194/egusphere-egu24-1322, https://doi.org/10.5194/egusphere-egu24-1322

Humlum, O., Stordahl, K. and Solheim, J.-E., 2013. The phase relation between atmospheric carbon dioxide and global temperature. Global and Planetary Change, v. 100, p. 51-69, https://doi.org/10.1016/j.gloplacha.2012.08.008

Inceoglu, F., Simoniello, R., Knudsen, M.F., Karoff, C., Olsen, J., Turck-Chiéze, S. and Jacobsen, B.H., 2015. Grand solar minima and maxima deduced from ^{10}Be and ^{14}C: magnetic dynamo configuration and polarity reversal. Astronomy & Astrophysics, v. 577, article A20, https://doi.org/10.1051/0004-6361/201424212

IPCC, 2013. Summary for policymakers. *In:* Stocker, T.F. and 9 others, eds., Climate Change 2013: The Physical Science Basis. Contribution of Working Group I to the Fifth Assessment Report of the Intergovernmental Panel on Climate Change.

Cambridge University Press, Cambridge UK and New York USA, p. 3-29, https://www.ipcc.ch/site/assets/uploads/2018/02/WG1AR5_SPM_FINAL.pdf

IPCC, 2014, Climate Change 2014, Synthesis Report: Contribution of Working Groups I, II and III to the Fifth Assessment Report of the Intergovernmental Panel on Climate Change: Geneva, IPCC, Geneva, Switzerland, 151 p, https://www.ipcc.ch/site/assets/uploads/2018/02/SYR_AR5_FINAL_full.pdf

IPCC, 2021a, Summary for policymakers. *In:* V. Masson-Delmotte, V. and 18 others, eds., Climate Change 2021: The Physical Science Basis. Contribution of Working Group I to the Sixth Assessment Report of the Intergovernmental Panel on Climate Change, Cambridge University Press, Cambridge UK and New York USA, p. 3-32, https://www.ipcc.ch/report/ar6/wg1/downloads/report/IPCC_AR6_WGI_SPM.pdf

IPCC, 2021b, Technical Summary. *In:* V. Masson-Delmotte, V. and 18 others, eds., Climate Change 2021: The Physical Science Basis. Contribution of Working Group I to the Sixth Assessment Report of the Intergovernmental Panel on Climate Change. Cambridge University Press, Cambridge UK and New York USA, p. 33-144, https://www.ipcc.ch/report/ar6/wg1/downloads/report/IPCC_AR6_WGI_TS.pdf

Kamis, J.E. and Kamis, P.E., 2016. Plate climatology theory. American Meteorological Society Annual Meeting, abstract (plus downloadable handout and manuscript), https://ams.confex.com/ams/96Annual/webprogram/Paper290033.html

Karamanev, D., 2021. Impact of anthropogenic heat emissions on global atmospheric temperature. Preprints 2021, 2021040729, https://www.preprints.org/manuscript/202104.0729/v1

Klotzbach, P.J., Pielke, R.A., Sr., Pielke, R.A., Jr., Christy, J.R. and McNider, R.T., 2009. An alternative explanation for differential temperature trends at the surface and in the lower troposphere. Journal of Geophysical Research, v. 114, article D21102, 8 p, https://doi.org/10.1029/2009JD011841

Kulmala, M., Nieminen, T., Chellapermal, R., Makkonen, R., Bäck, J. and Kerminen, V.-M., 2013. Climate feedbacks linking the increasing atmospheric CO2 concentration, BVOC emissions, aerosols and clouds in forest ecosystems. *In:* Niinemets, U. and Russell K. Monson, R.K. (eds.). Biology, Controls and Models of Tree Volatile Organic Compound Emissions, Springer, Dordrecht, p. 489-508, https://link.springer.com/chapter/10.1007/978-94-007-6606-8_17

Lacis, A.A., Schmidt, G.A., Rind, D. and Reto A. Ruedy, R.A., 2010. Atmospheric CO2: principal control knob governing Earth's temperature. Science, v. 330, p. 356-359, https://www.science.org/doi/10.1126/science.1190653

Le Mouël, J.L., Lopes, F. and Courtillot, V., 2020. Characteristic time scales of decadal to centennial changes in global surface temperatures over the past 150 years. Earth and Space Science, 7(e2019EA000671), https://doi.org/10.1029/2019EA000671

Lockwood, M., Stamper, R. and Wild, M.N., 1999. A doubling of the Sun's coronal magnetic field during the past 100 years. Nature, v. 399, p. 437-439, https://doi.org/10.1038/20867

Lohmann, U., Friebel, F., Kanji, Z.A., Mahrt, F., Mensah, A.A. and Neubauer, D., 2020. Future warming exacerbated by aged-soot effect on cloud formation. Nature Science, v. 13, p. 674-680, https://doi.org/10.1038/s41561-020-0631-0

Marcott, S.A., Shakun, J.D., Clark, P.U. and Mix, A.C., 2013. A reconstruction of regional and global temperature for the past 11,300 years. Science, v. 339, p. 1198-1201, https://doi.org/10.1126/science.1228026

Mahoney, A.R., Barry, R.G., Smolyanitsky, V. and Fetterer, F. 2008. Observed sea ice extent in the Russian Arctic, 1933–2006. Journal of Geophysical Research, v. 113, article 11005, 11 p, https://doi.org/10.1029/2008JC004830

Met Office (UK Meteorological Office) 2025. Global temperature. Webpage accessed 27th January 2025. https://climate.metoffice.cloud/temperature.html#content

Murray, J. and Heggie, D., 2016. From urban to national heat island: the effect of

anthropogenic heat output on climate change in high population industrial countries. Earth's Future, v. 4, p. 298-304, https://doi.org/10.1002/2016EF000352

NASA, 2011. Black carbon: a global presence (including video). Webpage accessed 22nd January 2025, https://svs.gsfc.nasa.gov/3844

NASA, 2016. Video: super HD view of global carbon dioxide. Webpage accessed 22nd January 2025, https://science.nasa.gov/resource/video-super-hd-view-of-global-carbon-dioxide/ also https://www.youtube.com/embed/1rZDJrVcie4

NASA, 2025. GISS surface temperature analysis (v4) graphs and plots. Webpage accessed 22nd January 2025, https://data.giss.nasa.gov/gistemp/graphs_v4/

Oulu (University of Oulu/Sodankylä Geophysical Observatory), 2025. Cosmic-ray chart 1964-2024. Webpage accessed 21st January 2025, https://cosmicrays.oulu.fi

OWD (Our World in Data, University of Oxford), 2025a. Energy mix (graphs). Webpage accessed 20th January 2025, https://ourworldindata.org/energy-mix

OWD (Our World in Data, University of Oxford), 2025b. Electricity production by source (graphs). Webpage accessed 20th January 2025, https://ourworldindata.org/electricity-mix

OWD (Our World in Data, University of Oxford), 2025c. Years of fossil fuel reserves left, 2020. Webpage accessed 26th January 2025, https://ourworldindata.org/grapher/years-of-fossil-fuel-reserves-left

PAGES2k, 2019. Consistent multidecadal variability in global temperature reconstructions and simulations over the Common Era. Nature Geoscience, v. 12, p. 643-649, https://doi.org/10.1038/s41561-019-0400-0

Rohde, R., 2015. 400 years of sunspot observations (chart). Webpage accessed 22nd January 2025, https://commons.wikimedia.org/wiki/File:Sunspot_Numbers.png

Rubino, A., Zanchettin, D., De Rovere, F. and Michael J. McPhaden, M.J. 2020. On the interchangeability of sea-surface and near-surface air temperature anomalies in climatologies. Nature Scientific Reports, 10:7433, https://doi.org/10.1038/s41598-020-64167-1

Shibata, Y., Nagasawa, C., Abo, M., Inoue, M., Morino, I. and Uchino, O., 2018. Comparison of CO2 vertical profiles in the lower troposphere between 1.6 μm differential absorption Lidar and aircraft measurements over Tsukuba. Sensors, v.18 (4064), https://www.mdpi.com/1424-8220/18/11/4064

Sigl, M. and 23 others, 2015. Timing and climate forcing of volcanic eruptions for the past 2,500 years. Nature, v. 523, p. 543-549, https://doi.org/10.1038/nature14565

Spencer, D.R., 2025. Satellite-based temperature of the global lower atmosphere. Webpage accessed 18th January 2025, https://www.drroyspencer.com/latest-global-temperatures/

Solanki, S.K., Usoskin, I.G., Kromer, B., Schüssler, M. and Beer, J., 2004. Unusual activity of the Sun during recent decades compared to the previous 11,000 years. Nature, v. 431, p. 1084-1087, https://doi.org/10.1038/nature02995

Steinhilber, F. and Beer, J., 2011. Solar activity – the past 1200 years. Past Global Changes Magazine, v. 19, p. 5-6, https://doi.org/10.22498/pages.19.1.5

Stephens, G.L., 2005. Cloud feedbacks in the climate system: a critical review. Journal of Climate, v. 18, p. 237-273. https://journals.ametsoc.org/view/journals/clim/18/2/jcli-3243.1.xml

Stroeve, J., Holland, M.M., Meier, W., Scambos, T. and Serreze, M., 2007. Arctic sea ice decline: faster than forecast. Geophysical Research Letters, v. 34, article L09501, 5 p, https://doi.org/10.1029/2007GL029703

Svensmark, H., 2007. Cosmoclimatology: a new theory emerges. Astronomy & Geophysics, v. 48, p. 1.18–1.24, https://doi.org/10.1111/j.1468-4004.2007.48118.x

Szopa, S. and 12 others, 2021. Chapter 6, Short-lived climate forcers. I*n:* Masson-Delmotte, V., and 18 others, eds., Climate Change 2021: The Physical Science Basis. Contribution of Working Group I to the Sixth Assessment Report of the Intergovernmental Panel on Climate Change: Cambridge University Press, Cambridge UK and New York USA, p. 817–922, https://www.ipcc.ch/report/ar6/wg1/downloads/report/IPCC_AR6_WGI_Chapter06.pdf

UAH (University of Alabama in Huntsville), 2025. Global temperature report: December 2024. Website accessed 21st January 2025, https://www.nsstc.uah.edu/climate/2024/December/GTR_202412DEC_v1.pdf

van Wijngaarden, W.A. and Happer, W., 2020. Dependence of Earth's thermal radiation on five most abundant greenhouse gases. ArXiv:2006.03098, 38p, https://arxiv.org/abs/2006.03098

Vinos, J., 2017, Nature Unbound III: Holocene climate variability (Part A). Webpage accessed 22nd January 2025, https://judithcurry.com/2017/04/30/

Vinther, B.M. and 13 others, 2009. Holocene thinning of the Greenland ice sheet. Nature, v. 461, p. 385-38, https://doi.org/10.1038/nature08355

Wigley, T.M.L., 2005. The climate change commitment. Science, v. 307, p. 1766-1769, https://doi.org/10.1126/science.1103934

Wikipedia, 2025a. 8.2-kiloyear event. Webpage accessed 18 January 2025, https://en.wikipedia.org/wiki/8.2-kiloyear_event

Wikipedia, 2025b. Global warming hiatus. Webpage accessed 18 January 2025, https://en.wikipedia.org/wiki/Global_warming_hiatus

Wu, C.J., Usoskin, I.G., Krivova, N., Kovaltsov, G.A., Baroni, M., Bard, E. and Solanki, S.K., 2018. Solar activity over nine millennia: a consistent multi-proxy reconstruction. Astronomy & Astrophysics, v. 615, article A93, 13 p, https://doi.org/10.1051/0004-6361/201731892

Zhang, X., Li, X., Chen, D., Cui, H. and Ge, Q., 2019. Overestimated climate warming and climate variability due to spatially homogeneous CO_2 in climate modeling over the Northern Hemisphere since the mid-19th century. Nature Scientific Reports, v. 9 (17426), https://doi.org/10.1038/s41598-019-53513-7

Zhao, X., Allen, R.J., Wood, T. and Maycock, A.C., 2020. Tropical belt width proportionately more sensitive to aerosols than greenhouse gases. Geophysical Research Letters, v. 7 (e2019GL086425), https://doi.org/10.1029/2019GL086425

Zheng, Y., Li, F., Hao, L., Shedayi, A.A., Guo, L., Ma, C., Huang, B. and Xu, M., 2018. The optimal CO2 concentrations for the growth of three perennial grass species. BMC Plant Biology, v. 18(27), https://link.springer.com/article/10.1186/s12870-018-1243-3